

Image Demosaicing: A Roadmap to Peculiarity Imaging

Gurjot Kaur Walia¹, Jagroop Singh Sidhu²

¹Research Scholar, Electronics and Communication Engineering, I. K. Gujral Punjab Technical University, Kapurthala, Punjab, India, 144603

²Associate Professor, Deptt. of ECE, DAVIET, Jalandhar, Punjab, India, 144021

Article History: Received: 11 January 2021; Revised: 27 February 2021; Accepted: 27 March 2021; Published online: 10 May 2021

Abstract: Image demosaicing is the process of reconstruction of full color image on the basis of various methods from the data samples obtained by acquisition devices. This paper deals with the various techniques that can be utilized to achieve demosaiced image by suitably classifying it into various categories. Moreover, it also provides an insight into the evaluation metrics used for confirming the performance of demosaicing techniques. Besides, the potential areas are also investigated for realistic applications where image demosaicing is found to be highly beneficial for healthcare and forensics.

Keywords: Image demosaicing, Bayer pattern, Learning-based algorithms, Medical imaging, Image forgery, Healthcare

1. Introduction

Owing to the rapid advancements in technology as well as the easy availability of digital cameras and mobile phones, the usage of images and videos has increased manifolds in the various regimes such as education, healthcare, surveillance, etc., [1-5]. Despite the technological advancements, there is still need to improve the quality of an image. Image quality is dependent on various factors ranging from features of cameras such as its resolution, sensitivity to light, sensor's dynamic range, etc. to the conditions that occur while capturing the images such as adjustment of white balance, focus adjustment, color interpolation, color correction, compression, etc. However, Color Filter Array (CFA) interpolation is an indispensable part of image pipeline which is used to recover full resolution image from its CFA data [6-8]. The requirement of CFA in color images is that there must be a minimum of three color samples at pixel location. One way is to use beam-splitters along the optical path, so as to project the image on all three sensors individually. Afterwards, color filter is placed before each sensor in order to obtain three color component images. It is challenging approach not only in terms of cost but also in alignment. Since, it needs three Charge Coupled Devices (CCD) sensors which need precise alignment that may otherwise lead to a phase delay. Another way is that the color sensors can be stacked on top of one another as in Foveon cameras [9] but it escalates the exposure time as the light requires penetrating the three Silicon levels. Hence, the most cost effective method is to use CFA before the sensor to acquire one color component at a pixel and then, restoring other two color components [10-11]. This process of reconstruction of a full color image from the single color component is commonly referred to as demosaicing. Although there are various CFA patterns but widely used Bayer pattern among them [8] is that where the green component is sampled by quincunx grid while red and blue components are attained using the rectangular grid. The density of the green components is two times the red and blue color components as the human eye is more sensitive to it. Several other CFA arrangements can also be used such as utilizing the subtractive primary colors cyan, magenta, and yellow (CMY), Emerald filter, cyan, magenta, yellow, and green (CMYG), panchromatic pixels, linear combination of red, green, and blue for decreasing aliasing introduced by the sampling, quantitative theory for optimal pattern that reduces the reconstruction error, etc. [12-15]. The presented work is generally focused on the reconstruction of images that can be obtained using CFA arrangement.

Image demosaicing is basically the reconstruction of the color image by utilizing the interpolation techniques that are especially devised to reconstruct the images sampled using a CFA otherwise it may lead to the artifacts such as false colors and zippering effect in some portions of an image, thereby reducing the image visual quality [12]. Moreover, most of these algorithms are complex, time-consuming and have high computational cost. It is worth noting that there is tradeoff between accuracy and computational cost for various image demosaicing algorithms. Thus, it is required that the demosaicing algorithms must be less prone to the artifacts, low computational cost as well as able to preserve the image resolution.

This paper is structured in the following manner: Section 2 provides a detailed analysis of the demosaicing algorithms. Section 3 provides various assessment parameters for the demosaicing algorithms. Section 4 provides the applications associated with it. Finally, the conclusion is presented in Section 5.

2. Image Demosaicing Methods

The plethora of image demosaicing approaches are available but they are broadly classified into six categories as depicted in Figure 1.

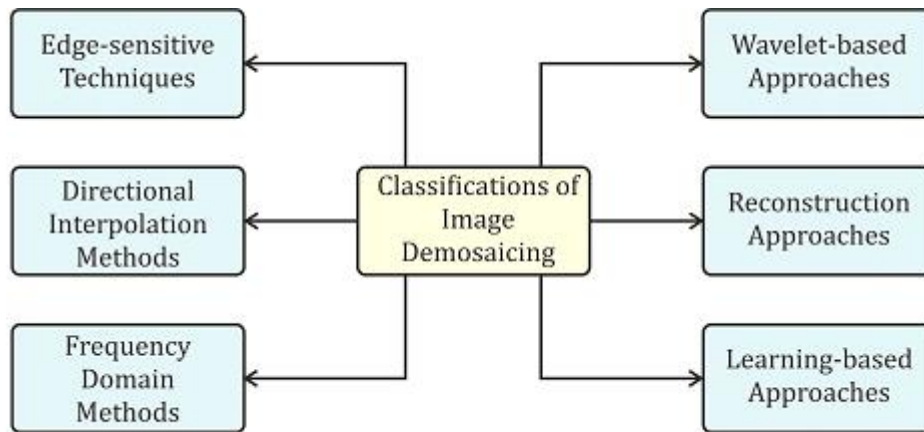


Figure 1 Categories of Image Demosaicing

2.1 Edge Sensitive Techniques

The accurate reconstruction of green color component is of utmost importance as its estimation is done prior to the red and blue components in a CFA image. If there is any error in reconstructing the green components, then it will further result in erroneous estimation of other two components. Hence, spectral correlation is utilized to increase the accuracy of green component reconstruction by utilizing the spatial correlation. Generally, it is the interpolation along edges by utilizing the color difference or color ratios for the reduction of color artifacts but the main challenge is to estimate the edge direction from CFA. In [16], bilinear interpolation is utilized for reconstructing the green component which is then employed for populating red and blue components by red to green and blue to green ratios. Usually, the color ratio approach is utilized but some techniques also utilized the difference in color components for reconstruction [17]. In [18] and [19], adaptive interpolation is utilized for interpolation along the edges. The gradient values are computed from the chrominance and luminance difference in horizontal and vertical directions of an image whose comparison is done with a threshold value for selecting the interpolation direction. By considering these methods, Laplacian operator based adaptive color plane interpolation method is proposed to determine the edge direction [20]. Kakarala and Baharav [21] presented Jacobian matrix and neighborhood voting based adaptive demosaicing method that requires less computation than existing algorithms. Lu and Tan [22] proposed a demosaicing method in which missing samples are estimated based on spectral and spatial correlation between the neighboring pixels. Moreover, it also employed adaptive median filter to suppress the demosaicing artifacts. Further, Gunturk et al. [23] provided an algorithm for reconstruction of color channels on the basis of observation of color samples as well as the previous knowledge of inter-channel correlation among the channels. The nonlinear iterative process reduced the interpolation artifacts. Nevertheless, Maschal et al. [24] presented two algorithms in which one algorithm works on the basis of computation of edge slope to measure accuracy of edge reconstruction while second is based on false color measure, thus, estimating the reconstruction of red and blue channel. Another spectral model [25] is proposed based on edge-sensing and post processing in imaging pipeline as universal demosaicing solution for preserving the color and sharpness of the captured image. In [26], median filter and spatial deinterlacing is utilised for estimating edges that provided accuracy along with suppression of artifacts. Furthermore, an adaptive approach [27] is used for estimating the green samples on the basis of variance of the color difference along the direction of edges that aids in reducing color artifacts while preserving the textural details. Based on color difference and weighted edge interpolation, an iterative demosaicing algorithm is presented in [28] for color channels estimation. In [29], Ferradans et al. are inspired by the concept of image inpainting to perform interpolation along image edges by level-set based geometric method. Moreover, regularization based methods are employed in [30, 31] for image demosaicing. These methods utilized the concept of prior knowledge about the smoothness of channel and correlation among color channels. In [7], heuristic algorithm is presented that utilized the weighted average based edge-directed technique for estimating the green channel. The second derivative based constraints as in [31] are utilized for updating other two channels. Lastly, all the channels are updated in an iterative manner in a method similar to the one presented in [32]. But, most edge-sensitive methods are either dependent on the direction of interpolation or weight estimation from CFA samples that may produce erroneous results because it contains less information as compared to the complete color image [33].

2.2 Directional Interpolation Techniques

In order to deal with the issues related to the edge-sensitive demosaicing methods, two estimations are made for the missing components and finally, the best decision is selected. In [34], the green color channel is reconstructed with the FIR filter in horizontal and vertical directions that are further utilized to estimate both red and blue channels with each green color component. The demosaiced image is selected from the two interpolated images on the basis of local homogeneity of an image, that is, the direction of interpolation which provides more

homogeneous neighborhood around the considered pixel is selected. However, the decision in [35] is done on the basis of directional reconstruction that preserved the maximum correlation in color gradients. The approaches described in [34, 35] involved the three color channels but an approach in [36] only estimated the best interpolation from the horizontal and vertical estimates of green channel and CFA samples. The missing red and blue components are then reconstructed based on their correlation with green channels. In another approach, the interpolation images obtained horizontally and vertically are fused and the image is reconstructed as the weighted sum of both the estimates [37, 38]. The weights are computed on the basis of linear minimum mean square error [37] and local polynomial approximation [38]. Pei and Tam in [39] proposed an efficient CFA interpolation approach with an image model that correlates the three color channels. In [40], an optimal direction for interpolation is estimated and hard decision interpolation is performed based on the spectral-spatial correlation concept. In [41], cubic spline interpolation and Taylor series based method is utilized in the four opposite directions to obtain the interpolants. The weighted median filter whose coefficients are determined from the edge orientation map is used to produce the output with the preserved edges. Chen et al. [42] presented an approach in which luminance component is estimated twice using bilinear interpolation that further assist in the final interpolation. In [43], missing color sample is estimated in numerous local directions and then fused in accordance with the local gradients. The adaptive thresholding is preferred over the nonlocal means filtering for improving the local estimate. In [44], the performance of interpolation is enhanced on the basis of higher correlation between the neighboring pixels in the eight directions. Further, the artifacts introduced during interpolation are reduced via color difference channels. Duran and Buades [45] suggested an approach based on the combination of various directionally interpolated images that are dependent on the chromatic smoothness. Then, NL means filtering is carried out that filtered the difference among color channels. In [46], demosaicing algorithm based on polynomial interpolation involving prediction of error and classification of edges is presented. After the prediction of missing components, its refinement is done for image enhancement and reduction of artifacts. Another interpolation approach that is widely used is based on the residual interpolation which is the difference between the observed and temporarily estimated pixel values. In [47, 48], the pixel values are temporarily estimated by minimizing the Laplacian energy of residuals while in [49, 50] adaptive method is used that involves both residual interpolation and the one defined in [47]. In another approach [51], hybrid algorithm based on residual interpolation and fuzzy edge strength is proposed for demosaicing. Initially, green channel is estimated on the basis of edge filter and fuzzy edge strength interpolation. Afterwards, red and blue channels are computed using residual interpolation by considering green channel to be a guide image.

2.3 Frequency domain methods

Some of the image demosaicing techniques also used frequency domain analysis. It generally involves the transformation of mosaic image into frequency domain while dividing an image into the frequency components that need to be corrected. Since, red and blue color channels are sampled at the lower rates, hence, some high frequency cannot be obtained by using standard techniques for interpolation. In order to resolve this issue, Glotzbach et al. suggested an interpolation method in [52] that uses high frequency information of green channel in combination with sub sampled red and blue images. Moreover, it also provides a way of reducing distortion due to aliasing. In [53], one-color per spatial position image is coded into luminance and chrominance of the corresponding three colors per spatial position image. The demosaicing is done by the spatial frequency filtering as specific arrangement is used by luminance and chrominance in the Fourier domain. However, due to aliasing between luminance and chrominance, it results in the artifacts that can be resolved by using a preprocessing filter. In [54], luminance is estimated for the channels by utilizing adaptive filtering technique. It is worth noting from the frequency analysis that high frequencies are more preserved if CFA image is sampled instead of filtering the color channels individually. Dubios proposed frequency domain based algorithms in [55] and [56]. Demosaicing is done by utilizing complementary asymmetric filters for estimating chrominance in [55] and least square filter design in combination with adaptive frequency domain method in [56]. However, in [57], luminance–chrominance based demosaicing algorithm is suggested that utilized low pass filter for the estimation of chrominance channel and then successively luminance channel is reconstructed. Edge information from low frequency components of luminance channel in combination with the adaptiveness is used for estimation. In [58], spatio-spectral sampling based method is utilized for the purpose of demosaicing. The spatial resolution is increased by specifying the required spatio-spectral response in Fourier domain in addition to the criteria required for optimization. However, Condat [59] suggested an approach for demosaicing with constraint that modulation of chrominance is done at a far distance from luminance in Fourier domain that is less sensitive to aliasing. In [60], frequency domain based CFA that includes constrained optimization for reducing the demosaicing error to provide effective results. The reformulation of optimization problem is done to reduce the number of parameters and improve the speed of searching parameters by selecting the geometric points on the surface or boundary of convex polyhedron or polygon. Another approach based on least-squares method for bandpass filters in frequency domain is suggested in [61]. However, in [62], the overlap between the frequency components of mosaicked images is minimized by multi-objective optimization technique where parameter is optimized on the basis of constrained optimization problem to reduce the visual artifacts.

2.4 Wavelet-based approaches

Some of the demosaicing employed Discrete Wavelet Transform (DWT) based on low pass and high pass filters for decomposing an image into four subbands, that is, LL, LH, HL, and HH. LL involves low pass filtering of both rows and columns; LH involves filtering of rows by low pass filter and columns by high pass filter; HL involves filtering of rows by high pass filter and columns by low pass filter while HH involves filtering of both rows and columns by high pass filter. It is a proven fact that these subbands are strongly correlated in different color channels, so, the information gathered from subbands in one color channel can be utilized for restoring the subbands in other channel [12]. In [23], there is high correlation between the high-frequency subbands that are decomposed using suitable wavelet basis. The reconstruction of image is done by using Projections Onto Convex Sets (POCS) approach by considering two constraints namely observation and detail constraint to ensure that interpolated data is consistent to the observed data and imposition of similar high frequency components in the different color channels. In [63], DWT is utilized for interpolation of three color channels to reduce zipper and aliasing effects. It employed wavelet coefficient interpolation for each channel and eventually combining them to obtain interpolated image. In a similar manner, Chen et al. [64] estimated the missing channel by utilizing the wavelet subbands where low frequency subband is computed using intra-channel data while high frequency subband is computed from the inter-channel data by considering the CFA pattern. In [65], wavelet transform is utilized for the demosaicing by combining the luminance image with interpolated R, G, and B images for enhancing spatial resolution in addition to preserving the color information. Moreover, in [66], a directional filtering based approach is used for locating the image details. But, its performance depends on the initial estimation in addition to high computational cost. It utilized wavelet transform for estimating the direction of edges from the luminance component of the image. Also, Zhang and Wu suggested that Mallat wavelet packet transform is successful in eradication of statistical redundancies in spatial as well as spectral domain [67]. In [68], hybrid demosaicing algorithm is presented that combined both frequency domain and wavelet decomposition for reduction of color artifacts near edges. However, Gaussian Scale Mixture (GSM) approach based on wavelets is suggested in [69] that aids in suppressing the zippering artifacts. Bayesian minimum mean square error estimation is used for the reconstruction of wavelet coefficients of luminance and chrominance channels whose correlation is effectively utilized in this algorithm.

2.5 Reconstruction approaches

Image reconstruction approaches are generally used for the purpose of demosaicing. Brainard [70] suggested optimum reconstruction algorithms based on Bayesian method for estimation to deal with issues related to polychromatic sampling. This approach is further extended in [71] by employing sharpening algorithm to suppress sharpness of an image that occurs when images are demosaiced. Mukherjee et al. [72] also presented a Bayesian approach along with Markov Random Field (MRF) that improves the quality of reconstructed image especially edges of an image. However, Linear Least Mean Squared Error (LLMSE) based demosaicing approach is employed for the reconstruction of image by considering frequency domain analysis in [73]. Further, Trussell and Hartwig [74] also presented Minimum Mean Square Error (MMSE) based estimator for demosaiced image. Similarly, LLMSE based method is suggested by Portilla et al. in [75] for estimation of joint spatial-chromatic covariance between color components which is further used for prediction of missing color components. However, the method is modified by stacking the notation of super pixels for effective computation of LMMSE [76]. In [77], a unified approach based on posteriori estimation by minimization of multiterm cost function and regularization by exploiting various constraints is suggested for super resolution and demosaicing. Another regularization based technique is proposed in [78] based on total variation criteria for imposing smoothness on color channels as well as color differences. Condat in [79] suggested iterative demosaicing approach involving minimization of variational function under consistency constraint. Moreover, it can be applied to noisy images on the basis of Lagrangian regularization. Further, Menon and Calvagno in [80] suggested regularization algorithm that utilized prior information of color images for demosaicing. The edges and other discontinuities of reconstructed image are improved by applying adaptive approach. In [81], image is reconstructed by interpolating the missing color components on the basis of minimization of regularization term with region-adaptive weights that avoided over-smoothness across edges of demosaiced images. However, edge information based nonlinear interpolation technique is suggested in [82] while image inpainting is utilized in [83] for reconstruction of edges in image. Further, an approach is developed in [84] to avoid artifacts by utilizing self-similarity of natural images for interpolating the missing components. Although spectral correlation aids in interpolation but weak correlations may result in large interpolation errors. To deal with this issue, hybrid approach involving MMSE and support vector regression is developed in [85]. Another approach based on compressive sensing is used for demosaicing by separately processing interchannel and interpixel correlations of an image [86]. Further, residual interpolation is utilized along with the error reduction approach in [87] for reducing error in reconstruction of edges while minimizing the color artifacts.

2.6 Learning based methods

Moreover, learning based techniques is also used in the image demosaicing from previous few years. Prakash et al. [6] performed the demosaicing operation by using a sparse model that is further optimized by the radial basis

function. In [88], Convolutional Neural Network (CNN) is used for demosaicing that involved construction of rough demosaiced image with color artifacts which is then refined by deep residual estimation and multi-model fusion. In [89-91] an approach is suggested to perform the task of both image denoising and demosaicing by utilizing the machine learning, CNN, and deep residual network that provided better details along with suppression of noise and artifacts. Moreover, an adaptive residual U-net is presented in [92] for the demosaicing application that further resulted in the reduction of artifacts in the textural area of an image. However, 3-stage CNN is presented in [93] in which the missing green channel components are reconstructed independently in first stage which is later on used for reconstructing the red and blue components and finally, high quality reconstruction of images is done in last stage. Although most of the learning techniques enhanced the performance but the high image quality is required. Hence, Generative Adversarial Network (GAN) is devised based on the U-net and dense residual network that efficiently eradicated the image artifacts [94]. Thus, learning based approaches are efficiently utilized for demosaicing purpose.

3. Evaluation Metrics for Demosaicing Algorithms

Generally, the demosaiced image is evaluated on the basis of MSE defined as the mean square of the difference between original and demosaiced image in each color defined as [34]:

$$MSE(z) = \frac{1}{MN} \sum_{m=1}^M \sum_{n=1}^N \left(\hat{I}_z(m, n) - I_z(m, n) \right)^2 \quad (1)$$

where \hat{I}_z and I_z refers to the color component in demosaiced and original image such that z can be R, G, or B. Similarly, MSE of a full color image is defined as [34]:

$$CMSE = \frac{1}{3MN} \sum_{m=1}^M \sum_{n=1}^N \left(\hat{I}_z(m, n) - I_z(m, n) \right)^2 \quad (2)$$

Further, PSNR and CPSNR are computed from MSE and CMSE respectively. PSNR is given as [34]:

$$PSNR(z) = 10 \log_{10} \left(\frac{255^2}{MSE(z)} \right) \quad (3)$$

CPSNR is computed in a similar manner by replacing MSE by CMSE in (3). Higher value of PSNR and CPSNR shows better performance of the demosaicing algorithm. Moreover, the evaluation is also done by considering the similarity measures, particularly, SSIM, FSIM, MSSIM. SSIM measures the similarity between the demosaiced and original image defined as [99]:

$$SSIM = \frac{(2\mu_I \mu_J + K_1)(2\sigma_I \sigma_J + K_2)}{(\mu_I^2 + \mu_J^2 + K_1)(\sigma_I^2 + \sigma_J^2 + K_2)} \quad (4)$$

where, μ_I and μ_J represent the mean intensities, σ_I and σ_J denotes the contrast while K_1 and K_2 represent the constants. Similarly, FSIM is computed as [100]:

$$FSIM = \frac{\sum_{z \in A} S_L(z) PC_k(z)}{\sum_{z \in A} PC_k(z)} \quad (5)$$

$$\text{where } S_L(z) = \left(\frac{2PC_I(z)PC_J(z)+T_1}{PC_I^2(z)+PC_J^2(z)+T_1} \right)^\alpha \left(\frac{2GM_I(z)GM_J(z)+T_2}{GM_I^2(z)+GM_J^2(z)+T_2} \right)^\beta$$

Here, PC and GM refer to phase congruency and gradient magnitude, T_1 and T_2 are stability constants. Additionally, $PC_k(z) = \max(PC_I(z), PC_J(z))$ where z represents local window position. It is worth noting that $\alpha = \beta = 1$. Moreover, its performance can also be evaluated in terms of computational cost and speed. Low complexity or computational cost and high speed leads to better demosaicing algorithm [97]. S-CIELab metric is the extension of CIELab metric in S-CIELab color space. CIELab metric is the mean error processed with all image pixels given by [34]:

$$\Delta E_{Lab}^* = \frac{1}{MN} \sum_{m=1}^M \sum_{n=1}^N D_{m,n} \quad (6)$$

where $D_{m,n} = \left\| \pi(I(m, n)) - \pi(\hat{I}(m, n)) \right\|$, that is, $\|\cdot\|$ indicates ℓ_2 norm. Lower the value of CIELab metric, better is the value of demosaicing quality. These evaluation metrics are mostly used in the demosaicing algorithms.

4. Applications of Demosaicing

The process of image demosaicing can be utilized in the various image processing applications such as in low light images, image forensics, polarization images, medical imaging, hardware platforms. The demosaicing is successfully employed in case of realistic images with low light environment in [98]. Further, the demosaicing techniques are also utilized for the application of image forensics, for instance, demosaicing artifacts can be used for the detection of forged images by analyzing these CFA artifacts [99-101]. Image demosaicing is also employed in the field of medical imaging [102, 103] that is one of the most important issues as compressed data in medical images can result in life-threatening conditions. Moreover, it is used in the polarization images which are used for analyzing the oscillation direction of electric field as per description of light [104]. Furthermore, demosaicing algorithm developed in [97] can be deployed on hardware that is capable of providing efficient performance.

5. Conclusion

In this paper, the issue of demosaicing is analyzed by focusing on the Bayer CFA pattern. The image demosaicing techniques based on various categories are explored in this paper. Further, learning based techniques are used for demosaicing in the recent work that provided promising results as compared to the traditional methods. Since, demosaicing often face the challenge of reducing the zipping and color artifacts. Hence, most of the techniques are aimed to reduce these artifacts for improving its performance. Additionally, demosaicing is also used in combination with denoising and super resolution by some of the techniques. Thus, unified algorithms can be used for performing multiple tasks with reduced complexity.

Acknowledgments

The author would like to thank Dean RIC, I. K. Gujral Punjab Technical University, Kapurthala and Principal, Guru Nanak Dev Engineering College, Ludhiana, for providing the necessary facilities to accomplish this work.

References

1. Boulos, M. N. K., Wheeler, S., Tavares, C., & Jones, R. (2011). How smartphones are changing the face of mobile and participatory healthcare: an overview, with example from eCAALYX. *Biomedical engineering online*, 10(1), 1-14.
2. Kaur, K., Kaur, G., & Kaur, J. (2017). Extraction of Abnormal Portion of Brain Using Jaya Algorithm. In *Proceedings of Sixth International Conference on Soft Computing for Problem Solving* (pp. 163-169). Springer, Singapore.
3. Kaur, D., &Walia, G. K. (2020). A Hybrid ACO-SVM Approach for Detecting and Classifying Malaria Parasites. In *Computational Network Application Tools for Performance Management* (pp. 139-152). Springer, Singapore.
4. Kumar, V. A., Kumar, V. A., Malathi, S., Vengatesan, K., & Ramakrishnan, M. (2018). Facial recognition system for suspect identification using a surveillance camera. *Pattern Recognition and Image Analysis*, 28(3), 410-420.
5. Kaur, K., Walia, G. K., & Kaur, J. (2018). Neural Network Ensemble and Jaya Algorithm Based Diagnosis of Brain Tumor Using MRI Images. *Journal of the Institution of engineers (India): Series B*, 99(5), 509-517.
6. Prakash, V. S., Prasad, K. S., & Prasad, T. J. C. (2017). Color image demosaicing using sparse based radial basis function network. *Alexandria Engineering Journal*, 56(4), 477-483.
7. Boccuto, A., Gerace, I., Giorgetti, V., & Rinaldi, M. (2019). A Fast Algorithm for the Demosaicing Problem Concerning the Bayer Pattern. *The Open Signal Processing Journal*, 6(1).
8. Bayer, B. E. (1976). U.S. Patent No. 3,971,065. Washington, DC: U.S. Patent and Trademark Office.
9. Hubel, P. M., Liu, J., &Guttosch, R. J. (2004, June). Spatial frequency response of color image sensors: Bayer color filters and Foveon X3. In *Sensors and Camera Systems for Scientific, Industrial, and Digital Photography Applications V* (Vol. 5301, pp. 402-407). International Society for Optics and Photonics.
10. Gunturk, B. K., Glotzbach, J., Altunbasak, Y., Schafer, R. W., &Mersereau, R. M. (2005). Demosaicking: color filter array interpolation. *IEEE Signal processing magazine*, 22(1), 44-54.
11. Li, X., Gunturk, B., & Zhang, L. (2008, January). Image demosaicing: A systematic survey. In *Visual Communications and Image Processing 2008* (Vol. 6822, p. 68221J). International Society for Optics and Photonics.
12. Menon, D., &Calvagno, G. (2011). Color image demosaicking: An overview. *Signal Processing: Image Communication*, 26(8-9), 518-533.
13. Hamilton Jr, J. F., & Compton, J. T. (2012). U.S. Patent No. 8,274,715. Washington, DC: U.S. Patent and Trademark Office.
14. Hirakawa, K., & Wolfe, P. J. (2008). Spatio-spectral color filter array design for optimal image recovery. *IEEE Transactions on Image Processing*, 17(10), 1876-1890.

15. Lu, Y. M., & Vetterli, M. (2009, January). Optimal color filter array design: Quantitative conditions and an efficient search procedure. In *Digital Photography V* (Vol. 7250, p. 725009). International Society for Optics and Photonics.
16. Cok, D. R. (1987). U.S. Patent No. 4,642,678. Washington, DC: U.S. Patent and Trademark Office.
17. Adams Jr, J. E. (1995, March). Interactions between color plane interpolation and other image processing functions in electronic photography. In *Cameras and Systems for Electronic Photography and Scientific Imaging* (Vol. 2416, pp. 144-151). International Society for Optics and Photonics.
18. Laroche, C. A., & Prescott, M. A. (1994). U.S. Patent No. 5,373,322. Washington, DC: U.S. Patent and Trademark Office.
19. Hibbard, R. H. (1995). U.S. Patent No. 5,382,976. Washington, DC: U.S. Patent and Trademark Office.
20. Hamilton Jr, J. F., & Adams Jr, J. E. (1997). U.S. Patent No. 5,629,734. Washington, DC: U.S. Patent and Trademark Office.
21. Kakarala, R., & Baharav, Z. (2002). Adaptive demosaicing with the principal vector method. *IEEE Transactions on Consumer Electronics*, 48(4), 932-937.
22. Lu, W., & Tan, Y. P. (2003). Color filter array demosaicking: new method and performance measures. *IEEE transactions on image processing*, 12(10), 1194-1210.
23. Gunturk, B. K., Altunbasak, Y., & Mersereau, R. M. (2002). Color plane interpolation using alternating projections. *IEEE transactions on image processing*, 11(9), 997-1013.
24. Maschal, R. A., Young, S. S., Reynolds, J. P., Krapels, K., Fanning, J., & Corbin, T. (2012). New image quality assessment algorithms for CFA demosaicing. *IEEE sensors journal*, 13(1), 371-378.
25. Lukac, R., & Plataniotis, K. N. (2005). Universal demosaicking for imaging pipelines with an RGB color filter array. *Pattern Recognition*, 38(11), 2208-2212.
26. Huang, W. T., Chen, W. J., & Tai, S. C. (2010). Color demosaicking using deinterlacing and median-based filtering techniques. *Journal of Electronic Imaging*, 19(4), 043018.
27. Chung, K. H., & Chan, Y. H. (2006). Color demosaicing using variance of color differences. *IEEE transactions on image processing*, 15(10), 2944-2955.
28. Su, C. Y. (2006). Highly effective iterative demosaicing using weighted-edge and color-difference interpolations. *IEEE Transactions on Consumer Electronics*, 52(2), 639-645.
29. Ferradans, S., Bertalmio, M., & Caselles, V. (2009). Geometry-based demosaicking. *IEEE Transactions on Image Processing*, 18(3), 665-670.
30. Menon, D., & Calvagno, G. (2009). Regularization approaches to demosaicking. *IEEE Transactions on Image Processing*, 18(10), 2209-2220.
31. Gerace, I., Martinelli, F., & Tonazzini, A. (2014, November). Demosaicing of noisy color images through edge-preserving regularization. In *2014 International Workshop on Computational Intelligence for Multimedia Understanding (IWCIM)* (pp. 1-5). IEEE.
32. Freeman, W. T. (1988). U.S. Patent No. 4,724,395. Washington, DC: U.S. Patent and Trademark Office.
33. Hirakawa, K., & Parks, T. W. (2005). Adaptive homogeneity-directed demosaicing algorithm. *Ieee transactions on image processing*, 14(3), 360-369.
34. Zhen, R., & Stevenson, R. L. (2015). Image demosaicing. In *Color image and video enhancement* (pp. 13-54). Springer, Cham.
35. Wu, X., & Zhang, N. (2004). Primary-consistent soft-decision color demosaicking for digital cameras (patent pending). *IEEE Transactions on Image Processing*, 13(9), 1263-1274.
36. Menon, D., Andriani, S., & Calvagno, G. (2006). Demosaicing with directional filtering and a posteriori decision. *IEEE Transactions on Image Processing*, 16(1), 132-141.
37. Zhang, L., & Wu, X. (2005). Color demosaicking via directional linear minimum mean square-error estimation. *IEEE Transactions on Image Processing*, 14(12), 2167-2178.
38. Paliy, D., Katkovnik, V., Bilcu, R., Alenius, S., & Egiazarian, K. (2007). Spatially adaptive color filter array interpolation for noiseless and noisy data. *International Journal of Imaging Systems and Technology*, 17(3), 105-122.
39. Pei, S. C., & Tam, I. K. (2003). Effective color interpolation in CCD color filter arrays using signal correlation. *IEEE Transactions on Circuits and Systems for video technology*, 13(6), 503-513.
40. Tsai, C. Y., & Song, K. T. (2006). Heterogeneity-projection hard-decision color interpolation using spectral-spatial correlation. *IEEE Transactions on Image Processing*, 16(1), 78-91.
41. Li, J. S. J., & Randhawa, S. (2009). Color filter array demosaicking using high-order interpolation techniques with a weighted median filter for sharp color edge preservation. *IEEE Transactions on Image Processing*, 18(9), 1946-1957.

42. Chen, W. G., Wang, X., & Xing, J. G. (2012). Colour demosaicking for complementary colour filter array using spectral and spatial correlations. *IET image processing*, 6(7), 901-909.
43. Zhang, L., Wu, X., Buades, A., & Li, X. (2011). Color demosaicking by local directional interpolation and nonlocal adaptive thresholding. *Journal of Electronic imaging*, 20(2), 023016.
44. Chen, X., He, L., Jeon, G., & Jeong, J. (2014). Multidirectional weighted interpolation and refinement method for Bayer pattern CFA demosaicking. *IEEE Transactions on Circuits and Systems for Video Technology*, 25(8), 1271-1282.
45. Duran, J., & Buades, A. (2014). Self-similarity and spectral correlation adaptive algorithm for color demosaicking. *IEEE transactions on image processing*, 23(9), 4031-4040.
46. Wu, J., Anisetti, M., Wu, W., Damiani, E., & Jeon, G. (2016). Bayer demosaicking with polynomial interpolation. *IEEE Transactions on Image Processing*, 25(11), 5369-5382.
47. Kiku, D., Monno, Y., Tanaka, M., & Okutomi, M. (2014, March). Minimized-Laplacian residual interpolation for color image demosaicking. In *Digital Photography X (Vol. 9023, p. 90230L)*. International Society for Optics and Photonics.
48. Kiku, D., Monno, Y., Tanaka, M., & Okutomi, M. (2016). Beyond color difference: Residual interpolation for color image demosaicking. *IEEE Transactions on Image Processing*, 25(3), 1288-1300.
49. Monno, Y., Kiku, D., Tanaka, M., & Okutomi, M. (2015, September). Adaptive residual interpolation for color image demosaicking. In *2015 IEEE International Conference on Image Processing (ICIP)* (pp. 3861-3865). IEEE.
50. Monno, Y., Kiku, D., Tanaka, M., & Okutomi, M. (2017). Adaptive residual interpolation for color and multispectral image demosaicking. *Sensors*, 17(12), 2787.
51. Sun, B., Yuan, N., & Zhao, Z. (2019). A Hybrid Demosaicking Algorithm for Area Scan Industrial Camera Based on Fuzzy Edge Strength and Residual Interpolation. *IEEE Transactions on Industrial Informatics*, 16(6), 4038-4048.
52. Glotzbach, J. W., Schafer, R. W., & Illgner, K. (2001, October). A method of color filter array interpolation with alias cancellation properties. In *Proceedings 2001 International Conference on Image Processing (Cat. No. 01CH37205) (Vol. 1, pp. 141-144)*. IEEE.
53. Alleysson, D., Susstrunk, S., & Héroult, J. (2005). Linear demosaicing inspired by the human visual system. *IEEE Transactions on Image Processing*, 14(4), 439-449.
54. Lian, N. X., Chang, L., Tan, Y. P., & Zagorodnov, V. (2007). Adaptive filtering for color filter array demosaicking. *IEEE Transactions on Image Processing*, 16(10), 2515-2525.
55. Dubois, E. (2005). Frequency-domain methods for demosaicking of Bayer-sampled color images. *IEEE Signal Processing Letters*, 12(12), 847-850.
56. Dubois, E. (2006, October). Filter design for adaptive frequency-domain Bayer demosaicking. In *2006 International Conference on Image Processing* (pp. 2705-2708). IEEE.
57. De Lavarène, B. C., Alleysson, D., Durette, B., & Héroult, J. (2007, September). Efficient demosaicing through recursive filtering. In *2007 IEEE International Conference on Image Processing (Vol. 2, pp. II-189)*. IEEE.
58. Hirakawa, K., & Wolfe, P. J. (2008). Spatio-spectral color filter array design for optimal image recovery. *IEEE Transactions on Image Processing*, 17(10), 1876-1890.
59. Condat, L. (2011). A new color filter array with optimal properties for noiseless and noisy color image acquisition. *IEEE Transactions on image processing*, 20(8), 2200-2210.
60. Hao, P., Li, Y., Lin, Z., & Dubois, E. (2010). A geometric method for optimal design of color filter arrays. *IEEE Transactions on Image Processing*, 20(3), 709-722.
61. Leung, B., Jeon, G., & Dubois, E. (2011). Least-squares luma-chromad multiplexing algorithm for Bayer demosaicking. *IEEE Transactions on Image Processing*, 20(7), 1885-1894.
62. Bai, C., Li, J., Lin, Z., & Yu, J. (2016). Automatic design of color filter arrays in the frequency domain. *IEEE Transactions on Image Processing*, 25(4), 1793-1807.
63. Spampinato, G., Bruna, A., Sanguedolce, G., Ardizzone, E., & La Cascia, M. (2005, March). Improved color interpolation using discrete wavelet transform. In *Image and Video Communications and Processing 2005 (Vol. 5685, pp. 753-760)*. International Society for Optics and Photonics.
64. Chen, L., Yap, K. H., & He, Y. (2005, September). Color filter array demosaicking using wavelet-based subband synthesis. In *IEEE International Conference on Image Processing 2005 (Vol. 2, pp. II-1002)*. IEEE.
65. Driesen, J., & Scheunders, P. (2004, October). Wavelet-based color filter array demosaicking. In *2004 International Conference on Image Processing, 2004. ICIP'04. (Vol. 5, pp. 3311-3314)*. IEEE.
66. Menon, D., & Calvagno, G. (2007, September). Demosaicing based on wavelet analysis of the luminance component. In *2007 IEEE International conference on image processing (Vol. 2, pp. II-181)*. IEEE.

67. Zhang, N., & Wu, X. (2006). Lossless compression of color mosaic images. *IEEE Transactions on Image Processing*, 15(6), 1379-1388.
68. Kolta, R. W. B., Aly, H. A., &Fakhr, W. (2011, November). A hybrid demosaicking algorithm using frequency domain and wavelet methods. In *2011 International Conference on Image Information Processing* (pp. 1-6). IEEE.
69. Zhang, J., Sheng, A., &Hirakawa, K. (2018). A Wavelet-GSM Approach to Demosaicking. *IEEE Signal Processing Letters*, 25(6), 778-782.
70. Brainard, D. H. (1994, May). Bayesian method for reconstructing color images from trichromatic samples. In *Proceedings of the IS&T 47th Annual Meeting* (pp. 375-380).
71. Longere, P., Zhang, X., Delahunt, P. B., &Brainard, D. H. (2002). Perceptual assessment of demosaicing algorithm performance. *Proceedings of the IEEE*, 90(1), 123-132.
72. Mukherjee, J., Parthasarathi, R., & Goyal, S. (2001). Markov random field processing for color demosaicing. *Pattern Recognition Letters*, 22(3-4), 339-351.
73. Taubman, D. (2000, September). Generalized wiener reconstruction of images from colour sensor data using a scale invariant prior. In *Proceedings 2000 International Conference on Image Processing (Cat. No. 00CH37101)* (Vol. 3, pp. 801-804). IEEE.
74. Trussell, H. J., &Hartwig, R. E. (2002). Mathematics for demosaicking. *IEEE Transactions on image processing*, 11(4), 485-492.
75. Portilla, J., Otaduy, D., &Dorransoro, C. (2005, September). Low-complexity linear demosaicing using joint spatial-chromatic image statistics. In *IEEE International Conference on Image Processing 2005* (Vol. 1, pp. 1-61). IEEE.
76. De Lavarène, B. C., Alleysson, D., &Hérault, J. (2007). Practical implementation of LMMSE demosaicing using luminance and chrominance spaces. *Computer Vision and Image Understanding*, 107(1-2), 3-13.
77. Farsiu, S., Elad, M., &Milanfar, P. (2005). Multiframe demosaicing and super-resolution of color images. *IEEE transactions on image processing*, 15(1), 141-159.
78. Saito, T., & Komatsu, T. (2008, March). Demosaicing method using the extended color total-variation regularization. In *Digital Photography IV* (Vol. 6817, p. 68170C). International Society for Optics and Photonics.
79. Condat, L. (2009, November). A generic variational approach for demosaicking from an arbitrary color filter array. In *2009 16th IEEE International Conference on Image Processing (ICIP)* (pp. 1625-1628). IEEE.
80. Menon, D., &Calvagno, G. (2009). Regularization approaches to demosaicking. *IEEE Transactions on Image Processing*, 18(10), 2209-2220.
81. Omer, O. A., & Tanaka, T. (2007, December). Image demosaicking based on chrominance regularization with region-adaptive weights. In *2007 6th International Conference on Information, Communications & Signal Processing* (pp. 1-5). IEEE.
82. Muresan, D. D., & Parks, T. W. (2005). Demosaicing using optimal recovery. *IEEE Transactions on Image Processing*, 14(2), 267-278.
83. Ferradans, S., Bertalmio, M., &Caselles, V. (2009). Geometry-based demosaicking. *IEEE Transactions on Image Processing*, 18(3), 665-670.
84. Buades, A., Coll, B., Morel, J. M., &Sbert, C. (2009). Self-similarity driven color demosaicking. *IEEE Transactions on Image Processing*, 18(6), 1192-1202.
85. Zhang, F., Wu, X., Yang, X., Zhang, W., & Zhang, L. (2009). Robust color demosaicking with adaptation to varying spectral correlations. *IEEE Transactions on Image Processing*, 18(12), 2706-2717.
86. Moghadam, A. A., Aghagolzadeh, M., Kumar, M., &Radha, H. (2013). Compressive framework for demosaicing of natural images. *IEEE transactions on image processing*, 22(6), 2356-2371.
87. Asiq, M. S., & Emmanuel, W. S. (2019). Efficient colour filter array demosaicking with prior error reduction. *Journal of King Saud University-Computer and Information Sciences*.
88. D. S. Tan, W. Chen, and K. Hua, "Deepdemosaicking: Adaptive image demosaicking via multiple deep fully convolutional networks," *IEEE Transactions on Image Processing*, vol. 27, no. 5, pp. 2408–2419, 2018.
89. Khashabi, D., Nowozin, S., Jancsary, J., & Fitzgibbon, A. W. (2014). Joint demosaicing and denoising via learned nonparametric random fields. *IEEE Transactions on Image Processing*, 23(12), 4968-4981.
90. Satya, V., Prasad, K. S., & Prasad, T. J. (2017). Deep learning approach for image denoising and image demosaicing. *Int. J. Comput. Appl*, 168(9), 18-26.
91. Tan, H., Xiao, H., Lai, S., Liu, Y., & Zhang, M. (2018). Deep residual learning for image demosaicing and blind denoising. *Pattern Recognition Letters*, 2018.
92. Shopovska, I., Jovanov, L., & Philips, W. (2018, November). RGB-NIR demosaicing using deep residual U-Net. In *2018 26th Telecommunications Forum (TELFOR)* (pp. 1-4). IEEE.

93. Cui, K., Jin, Z., & Steinbach, E. (2018, October). Color image demosaicking using a 3-stage convolutional neural network structure. In 2018 25th IEEE International Conference on Image Processing (ICIP) (pp. 2177-2181). IEEE.
94. Kokkinos, F., & Lefkimmiatis, S. (2018). Deep image demosaicking using a cascade of convolutional residual denoising networks. In Proceedings of the European Conference on Computer Vision (ECCV) (pp. 303-319).
95. Gharbi, M., Chaurasia, G., Paris, S., & Durand, F. (2016). Deep joint demosaicking and denoising. *ACM Transactions on Graphics (TOG)*, 35(6), 1-12.
96. Ni, Z., Ma, K. K., Zeng, H., & Zhong, B. (2020). Color Image Demosaicing Using Progressive Collaborative Representation. *IEEE Transactions on Image Processing*, 29, 4952-4964.
97. Tang, J., Li, J., & Tan, P. (2021). Demosaicing by Differentiable Deep Restoration. *Applied Sciences*, 11(4), 1649.
98. Luo, J., & Wang, J. (2020). Image Demosaicing based on generative adversarial network. *Mathematical Problems in Engineering*, 2020.
99. Wang, Z., Bovik, A. C., Sheikh, H. R., & Simoncelli, E. P. (2004). Image quality assessment: from error visibility to structural similarity. *IEEE transactions on image processing*, 13(4), 600-612.
100. Zhang, L., Zhang, L., Mou, X., & Zhang, D. (2011). FSIM: A feature similarity index for image quality assessment. *IEEE transactions on Image Processing*, 20(8), 2378-2386.
101. Yang, X., Zhou, W., & Li, H. (2020). MCFD: A Hardware-efficient Noniterative Multicue Fusion Demosaicing Algorithm. *IEEE Transactions on Circuits and Systems for Video Technology*.
102. Kwan, C., Larkin, J., & Budavari, B. (2020, April). Demosaicing images in low lighting environments. In *Signal Processing, Sensor/Information Fusion, and Target Recognition XXIX* (Vol. 11423, p. 1142316). International Society for Optics and Photonics.
103. Cao, H., & Kot, A. C. (2009). Accurate detection of demosaicing regularity for digital image forensics. *IEEE Transactions on Information Forensics and Security*, 4(4), 899-910.
104. Singh, A., Singh, G., & Singh, K. (2018). A Markov based image forgery detection approach by analyzing CFA artifacts. *Multimedia Tools and Applications*, 77(21), 28949-28968.
105. Le, N., & Reiraint, F. (2019). An improved algorithm for digital image authentication and forgery localization using demosaicing artifacts. *IEEE Access*, 7, 125038-125053.
106. Parvathy, R., & Kumar, R. R. (2012, December). Demosaicing: Study and application in cytology image analysis. In 2012 Annual IEEE India Conference (INDICON) (pp. 781-784). IEEE.
107. Ramji, D. R., Palagan, C. A., Nithya, A., Appathurai, A., & Alex, E. J. (2020). Soft computing based color image demosaicing for medical Image processing. *Multimedia Tools and Applications*, 79(15), 10047-10063.
108. Facchini, G., Ceccarelli, L., Tomà, P., & Bartoloni, A. (2020). Recent imaging advancements for lung metastases in children with sarcoma. *Current Medical Imaging*.
109. Zhou, G., Hu, H., & Ma, L. (2017). Progress and review of 3D image feature reconstruction. *Recent Patents on Computer Science*, 10(1), 43-52.
110. Mihoubi, S., Lapray, P. J., & Bigu e, L. (2018). Survey of demosaicking methods for polarization filter array images. *Sensors*, 18(11), 3688.